Roberto Flórez Ablan

Collective effects in biphoton generation of a four-wave-mixing process

São Carlos

2022

Roberto Flórez Ablan

Collective effects in biphoton generation of a four-wave-mixing process

Undergraduate thesis presented to the Universidade Federal de São Carlos, Departamento de Física, as a necessary requirement to obtain the Bachelor's degree in Physics

Universidade Federal de São Carlos

Departamento de Física

Advisor: Romain Pierre Marcel Bachelard

São Carlos

2022

A mis padres, Elvira y Julio,
mis hermanos Julia, Diego y Fabricio,
mi tia Isa y mis abuelos Juan y Rosa
cuyo apoyo y amor transciende fronteras.

Acknowledgements

I am very grateful for all the opportunities that Brazil has given me for academic and personal growth. I would like to thank the Brazilian Ministry of External Relations (MRE) and the Ministry of Education (MEC) which support the existence of the PEC-G agreement and therefore the reason that I am finishing the present work. Moreover, I would like to thank all of my professors at UFSCar that without a doubt have positively changed my life. I will try my best to contribute back everything that Brazil and UFSCar have given me.

I would like to thank my parents Elvira and Julio, for their financial and emotional support throughout my life, without them I would not be here. My brothers Julia and Diego for our friendship and advices in my adaptation at UFSCar. My aunt Isa, for her care and contagious love of mathematics. Furthermore, I would like to thank my uncle Leandro, for introducing me to Python, and my aunt Magdiel, for always being very interested in all my projects and discussing them with me.

Also, I am very grateful for the affection, support, and care of my friends Milena, Karen, Andrés, Juscelio, Leandro, and Igor, they have taught me a lot and made my time at UFSCar so happy.

Specially, I thank Milena for all her love, care, and patience these last years, whose partnership has been a strength in difficult times.

Also, I would like to thank my buddies Moysés, Gabriel, Matheus, Victor, Hugo, and Edson for all the fun we have had together these years.

Furthermore, I would like to thank my advisor, Romain, for trusting me with this research project and being so present and helpful over its course. His way of doing science is inspiring. My learnings in this brief time completely exceeded all my expectations. Also, I would like to thank my first advisor Yara, for giving me my first scientific research project.

Moreover, I am very grateful to be part of the light-atom/quantum-many-body group, especially for having such a jovial atmosphere, as Isaac Asimov would put it[1]. I would like to specially thank André for his helpfulness and sympathy during the project, particularly at the beginning of the research with his technical assistance with the initial abstract and presentation, the first exact simulations, and the computational cluster. Analogously, I would like to thank Alan for his patience and help, particularly with all my doubts about the approximated approach. Moreover, I would like to thank Patricia for doing a thorough revision of the thesis.

The study presented on this theses was financed by scholarship No. 2021/04564-2 from the São Paulo Research Foundation (FAPESP). All the simulations shown in this work were done using the UFSCar HPC cluster.

Abstract

The generation of biphotons remains an important field of research, as several applications require such sources. For instance, some of their properties are fundamental in quantum communication, quantum computing, and quantum imaging.

Pairs of spatially correlated photons can be generated using four-wave-mixing (FWM) processes, taking advantage of the third-order nonlinear susceptibility χ^3 effect. A FWM configuration consists of two counter-propagating excitation fields acting on a cold atomic cloud which spontaneously generates pairs of photons in opposite directions through the nonlinear effect. Current theoretical models used to explain FWM in two-level systems have disregarded atomic interactions and considered an independent atom approach. Nevertheless, recent experiments have shown evidence of collective (superradiant) behavior in these types of systems.

In this context, we seek to understand the contributions of dipole-dipole interactions in the generation of biphotons. To this end, we propose to use an ab initio model to describe FWM in cold atomic clouds, where dipole-dipole interactions are accounted for. Our exact simulations with $N = 7$ atoms are compatible with the results from recent experiments. Furthermore, to simulate systems with a larger number of particles we derived and implemented a new scheme considering exclusively the single- and double-excitation subspace that is able to simulate systems of more than $N = 100$ scatterers.

Keywords: Four-wave-mixing, biphotons, collective effects.

List of Figures

Contents

1 Introduction

Emissions of spatially and temporally correlated photons (biphotons) have attracted much interest in recent years, since they are central to many quantum technologies. As carriers of quantum information, such sources are fundamental for large-scale quantum communications networks [3]. Also, correlated photons are very relevant in quantum teleportation [4], security [5], and imaging [6, 7].

Biphotons are typically generated via spontaneous parametric down-conversion (SPDC) using nonlinear crystals [8, 9]. However, photons generated this way are problematic for large-scale fiber optical communications because they show a large bandwidth (THz), and short coherence time (ps) and length (μm) [10]. On the other hand, another technique that can produce pairs of correlated photons and does not have the aforementioned limitations, is the four-wave-mixing (FWM) process.

FWM in two-level systems (TLS) has been used to produce pairs of photons for many groups during the last decade [11, 12, 13, 14, 15]. It consists of two counter-propagating excitation fields acting on an ensemble of cold two-level atoms. In the cloud, a third-order nonlinear susceptibility effect χ^3 comes up, which allows for the generation of spatially and temporally correlated photons in opposite directions. Typically, this process has been physically described as a vapor of **independent** [16, 17] atoms interacting via dipole interaction with the quantized electromagnetic field. However, last year, a experiment done in Recife (Brazil) [2] demonstrated evidence of collective behavior (i.e. superradiance-like decay rate) in FWM in TLS. Furthermore, other experiments done in similar conditions [11, 18, 19] also showed these effects. Such experimental observations of collective effects, suggest the existence of interactions between the scatterers in the atomic cloud.

In this context, the objective of our research is **to identify and characterize collective effects in FWM, considering N two-level atoms interacting through coupled dipoles interaction**.

To understand cooperative effects in atomic systems, it is interesting to first describe the case of spontaneous emission. Consider an excitation field of wavelength λ being applied on an ensemble of N excited two-level atoms, each particle having a natural decay rate of Γ_0. If the typical distances between the atoms are larger than λ, each particle scatters light by its own, ignoring the presence of other scatterers. In this situation, the radiated intensity is proportional to N and the system's decay rate is proportional to $e^{-\Gamma_0 t}$ (Figure 1(a)).

On the other hand, when the separation between the atoms is comparable or smaller

to λ, collective effects [20] arise [1]. Cooperative interference between the atoms changes the decay rate of the ensemble and the total radiated intensity. In the case of superradiance, there is a burst, proportional to N^2, and an enhanced decay rate proportional to $e^{-N\Gamma_0 t}$ (Figure 1(b)).

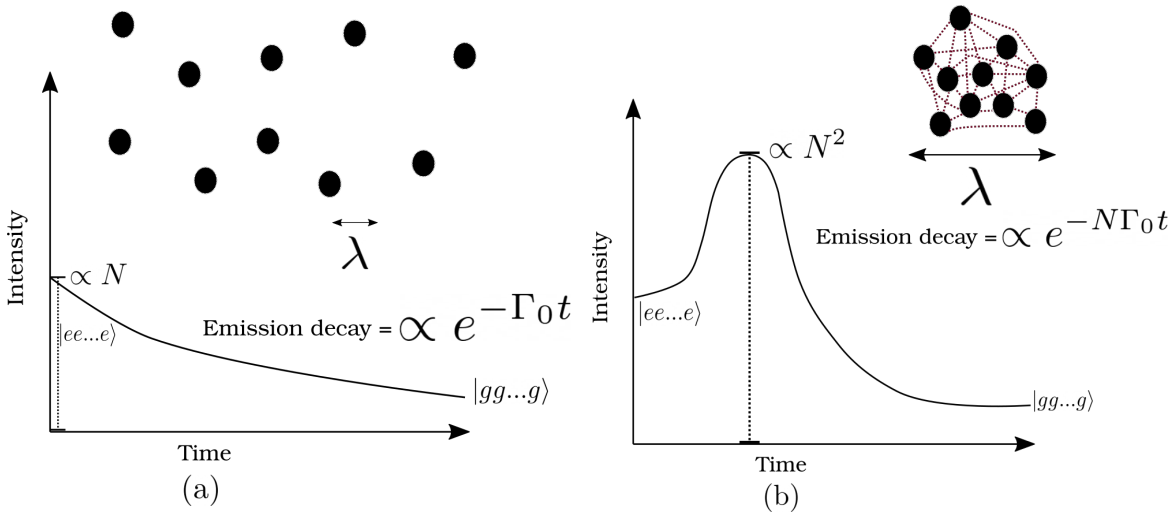

Figure 1 – Radiated intensity of an ensemble of N atoms as a function of time for the cases of (a) spontaneous emission and (b) superradiance.

In fact, it was precisely this enhancement in the decay rate that was reported in the Recife experiment [2]. They observed faster decay in the second correlation function (see Section 2.1.3) than what was expected by the independent atom approach. To account for this novel behavior, an empirical fit modification of the theoretical function originally proposed by Refs. [16, 17] was employed. In Section 3, we also compare this empirical fit with our results.

This thesis is organized as follows. Chapter 2 describes our exact (Section 2.1) and approximated (Section 2.2) models to describe the atomic system. Chapter 3 shows our simulations results and benchmarkings. At last, Chapter 4 is dedicated to the final remarks and future perspectives.

[1] Notice that the true spatial dependency of collective effects is not with the atomic density as described here but with the optical density $b_0 = \frac{2N}{(kr)^2}$

2 Dipole-dipole interactions model

2.1 Exact dynamics

2.1.1 Vector light model

Our theoretical model consists of a random cloud of N fixed two-level atoms excited by two counter-propagating fields with linear polarization. The particles interact only through light-induced dipole-dipole interactions. Our description closely follows Ref. [21]. We consider that the two pumps have the same Rabi frequency Ω and are detuned from the atomic resonant frequency ω_0 by Δ.

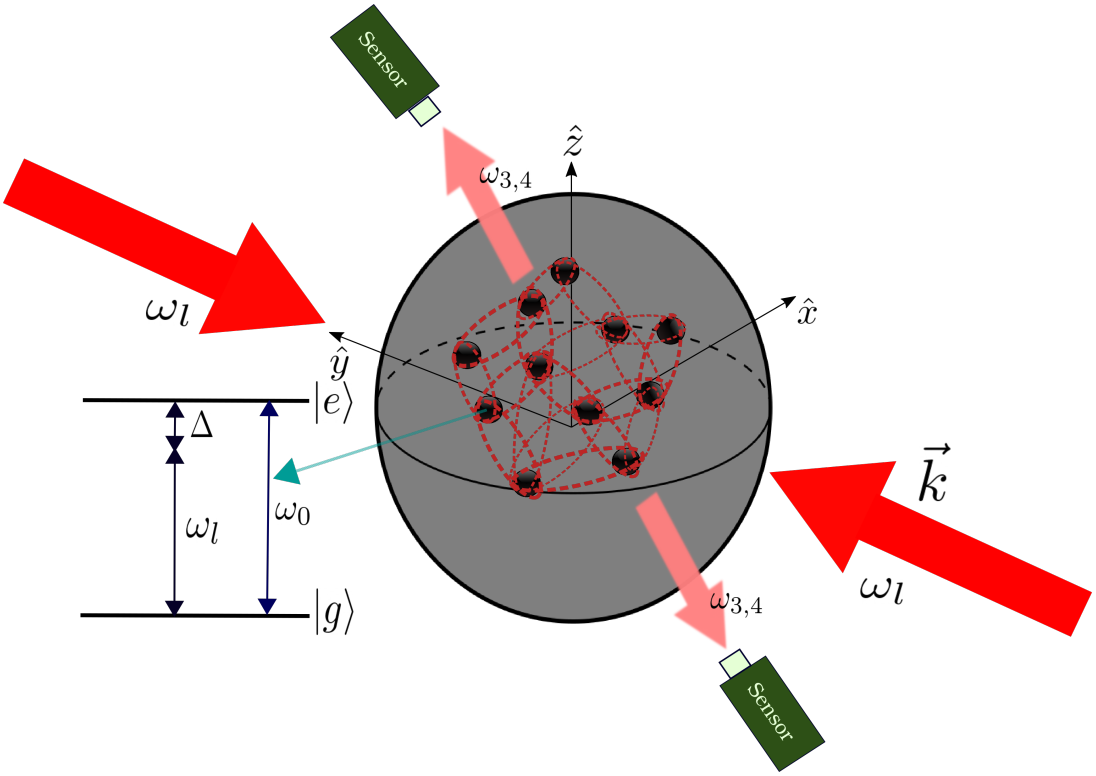

Figure 2 – Pictorical representation of FWM in TLS: dipole-dipole approach

Their dynamics is described considering Markov and rotating-wave approximations by a quantum master equation of the form ($\hbar \equiv 1$):

$$\frac{d}{dt}\hat{\rho} = \mathcal{H}(\hat{\rho}) + \mathcal{L}(\hat{\rho}) = -\mathrm{i}[\hat{H}, \hat{\rho}] + \mathcal{L}(\hat{\rho}), \tag{2.1}$$

where $\hat{\rho}$ is the density matrix operator, and the Hamiltonian and Lindblandian, respectively, are:

$$\begin{aligned}\hat{H} &= \hat{H}_{atom} + \hat{H}_{field_1} + \hat{H}_{field_2} + \hat{H}_{interaction} \\ &= -\Delta \sum_i \hat{\sigma}_i^+ \hat{\sigma}_i^- + \frac{1}{2}\sum_i \left(\Omega e^{i\mathbf{k}\cdot\mathbf{r}_i}\hat{\sigma}_i^+ + \text{H.c.}\right) + \frac{1}{2}\sum_i \left(\Omega e^{-i\mathbf{k}\cdot\mathbf{r}_i}\hat{\sigma}_i^+ + \text{H.c.}\right) + \sum_{i,j\neq i}\Delta_{ij}\hat{\sigma}_i^+\hat{\sigma}_j^-.\end{aligned} \tag{2.2}$$

$$\mathcal{L}(\hat{\rho}) = \frac{1}{2}\sum_{m,n}\Gamma_{mn}\left(2\hat{\sigma}_m^-\hat{\rho}\hat{\sigma}_n^+ - \left\{\hat{\sigma}_n^+\hat{\sigma}_m^-, \hat{\rho}\right\}\right). \tag{2.3}$$

We have introduced $\Delta_{ij} \equiv -\hat{\epsilon}_i^* \cdot \text{Re}\{\mathbf{G}_{ij}\} \cdot \hat{\epsilon}_j$ and $\Gamma_{ij} \equiv \hat{\epsilon}_i^* \cdot 2\text{Im}\{\mathbf{G}_{ij}\} \cdot \hat{\epsilon}_j$. They represent the elastic and inelastic terms of the dipolar interaction. The symbol $\hat{\epsilon}_i$ is the polarization of the ith dipole that we take $\hat{\epsilon}_i = \hat{\epsilon} = \hat{z}$. Also, $\sigma_i^\pm$ represent the atomic raising and lowering operators (for ground $|g\rangle$ and excited $|e\rangle$ state),

$$\begin{aligned}\sigma_i^+ &= |g_1\rangle \otimes ... \otimes |e_i\rangle \otimes ... \otimes |g_N\rangle\langle g_1| \otimes ... \otimes \langle g_i| \otimes ... \otimes \langle g_N| = |e_i\rangle\langle g_i|, \\ \sigma_i^- &= |g_i\rangle\langle e_i|.\end{aligned}$$

The effective potential between atoms i and j is given by the Green's tensor [22, 23, 24, 25]:

$$\mathbf{G}_{ij} \equiv \mathbf{G}(\mathbf{r}_{ij}) = \left(\frac{3\Gamma}{4}\frac{e^{ikr_{ij}}}{(kr_{ij})^3}\left[\left(k^2r_{ij}^2 + ikr_{ij} - 1\right)1_3 - \left(k^2r_{ij}^2 + i3kr_{ij} - 3\right)\frac{\mathbf{r}_{ij}\mathbf{r}_{ij}^T}{r_{ij}^2}\right]\right) \tag{2.4}$$

for $i \neq j$, where $\mathbf{r}_{ij} \equiv \mathbf{r}_i - \mathbf{r}_j$, and $\mathbf{G}_{ii} = i(\Gamma/2)1_3$ for the single-atom term, with $\Gamma_0 = d_0^2k^3/3\pi\epsilon_0\hbar$ denoting the single-atom spontaneous decay rate, ϵ_0 free space electric permittivity, d_0 the transition dipole moment, and $k = \omega_0/c = 2\pi/\lambda$ its wave number. We have taken the field propagation direction to be $\mathbf{k} = k\hat{y}$.

2.1.2 Scalar light model

Besides the vector light model explained in the previous section, we have also implemented the scalar light approximation [26]. In this model, we disregard effects due to the polarization of light and can simply take, $\Gamma_{ij} = 2\sin(kr_{ij})/kr_{ij}$ and $\Delta_{ij} = -\cos kr_{ij}/kr_{ij}$

2.1.3 Scattered light statistics

In the context of FWM, we have an especial interest in biphoton emissions, looking at the scattered light statistics by means of the second-order coherence function. This quantity measures the probability of two photons at positions $\mathbf{R}_1$ and $\mathbf{R}_2$ being detected with a time difference τ [27, 28]:

$$g^{(2)}_{\mathbf{R}_1,\mathbf{R}_2}(\tau) \equiv \lim_{t\to\infty}\frac{\left\langle \hat{E}^-(\mathbf{R}_1,t)\hat{E}^-(\mathbf{R}_2,t+\tau)\hat{E}^+(\mathbf{R}_2,t+\tau)\hat{E}^+(\mathbf{R}_1,t)\right\rangle}{\left\langle \hat{E}^-(\mathbf{R}_1,t)\hat{E}^+(\mathbf{R}_1,t)\right\rangle\left\langle \hat{E}^-(\mathbf{R}_1,t)\hat{E}^+(\mathbf{R}_2,t)\right\rangle} \tag{2.5}$$

where we have considered normal ordering. The scattered electric field is described in the far-field approximation and in a given direction $\hat{n}$, by

$$\hat{E}^{\pm} \sim \sum_{j=1}^{N} e^{\mp ik\hat{n}\cdot\mathbf{r}_j}\hat{\sigma}_j^{\mp}. \tag{2.6}$$

Also, an important quantity to characterize the scattered light statistics is the Cauchy-Schwartz inequality. This function is smaller than 1 for classical fields and read as

$$R(\tau) = \frac{\bar{g}_{\mathbf{R}_1,\mathbf{R}_2}(\tau)\bar{g}_{\mathbf{R}_1,\mathbf{R}_2}(\tau)}{\bar{g}_{\mathbf{R}_1,\mathbf{R}_1}(0)\bar{g}_{\mathbf{R}_2,\mathbf{R}_2}(0)} \leq 1. \tag{2.7}$$

2.2 Single and double excitation subspace dynamics

2.2.1 Analytical approach

The complete Hilbert space of our system has size $2^N \times 2^N$. Thus, we are only able to simulate exact systems of $N \leq 7$ atoms (128×128 matrices) before facing memory issues in our cluster. To overcome this problem, we follow an analytical approach only considering the subspace of single and double excited states.

Let us consider the following coefficients

$$\beta_\ell(t) = \left\langle \sigma_\ell^- \right\rangle = \mathrm{tr}\left\{\rho(t)\sigma_\ell^-\right\} \quad \text{and} \quad \beta_{k\ell}(t) = \left\langle \sigma_k^-\sigma_\ell^- \right\rangle = \mathrm{tr}\left\{\rho(t)\sigma_k^-\sigma_\ell^-\right\}.$$

The squared modulus of these quantities corresponds, respectively, to the probability that atom ℓ is excited (and no photon in the field) and the probability that atom k and atom ℓ are excited (and no photons in the field). Using Equation 2.1, calculating the commutation relations and considering that the number of atoms N in the system is much larger than the number of atomic excitations N_{exc} (weak-drive regime), we obtain the following system of differential equations [1]:

$$\dot{\beta}_t(t) = \left(i\Delta_\ell - \frac{\Gamma_{\ell\ell}}{2}\right)\beta_t(t) - \frac{i}{2}\Omega_t - \sum_{m\neq\ell}^{N} G_{tm}\beta_m(t) \tag{2.8}$$

$$\begin{aligned}\dot{\beta}_{k\ell}(t) = \left[i\left(\Delta_k + \Delta_\ell\right) - \frac{1}{2}\left(\Gamma_{kk} + \Gamma_{\ell\ell}\right)\right]\beta_{k\ell}(t) - \frac{i}{2}\left(\Omega_t\beta_k(t) + \Omega_k\beta_\ell(t)\right) \\ - \sum_{m\neq\ell}^{N} G_{\ell m}\beta_{km}(t) - \sum_{m\neq k}^{N} G_{km}\beta_{mt}(t)\end{aligned} \tag{2.9}$$

where $G_{\ell m} = \Gamma_{\ell m}/2 + i\Delta_{\ell m}$. Furthermore, our main objective is to obtain the scattered light statistics, so, using Equation 2.5 we calculate the expression for $g^{(2)}(0)$. The expectation

[1] Full derivation is available on Appendix B

value of the far-field $E^{\pm}$ operators are written using the single and double excitation state[1] and are simplified in terms of the β coefficients. We find:

$$g^{(2)}_{\mathbf{R}_1,\mathbf{R}_2}(0) =$$

$$\lim_{t\to\infty} \frac{\sum_{l\bar{L}m\bar{M}} e^{-ik(\hat{n}_2(\mathbf{r}_l-\mathbf{r}_{\bar{L}}))+\hat{n}_1(\mathbf{r}_m-\mathbf{r}_{\bar{M}}))}\beta_{l,m}(t)\beta^*{}_{\bar{L},\bar{M}}(t)}{\sum_{l\bar{L}} e^{-ikn_1(\mathbf{r}_l-\mathbf{r}_{\bar{L}})}\left(\beta_l(t)\beta^*{}_{\bar{L}}(t)+\sum_j 4\beta_{l,j}(t)\beta^*{}_{\bar{L},j}(t)\right)\sum_{l\bar{L}} e^{-ikn_2(\mathbf{r}_l-\mathbf{r}_{\bar{L}})}\left(\beta_l(t)\beta^*{}_{\bar{L}}(t)+\sum_j 4\beta_{l,j}(t)\beta^*{}_{\bar{L},j}(t)\right)}. \tag{2.10}$$

3 Results

3.1 Exact simulations

We have implemented the exact scalar and vector light models described previously (using QuTiP [29]) to investigate numerically the generation of biphotons. For each calculation, a different random set of atomic positions was generated. The simulations shown in this report are the result of the geometric average of many different atomic configurations (at least 200). Overall, our calculations with $N = 7$ atoms are consistent with recent experimental observations [2].

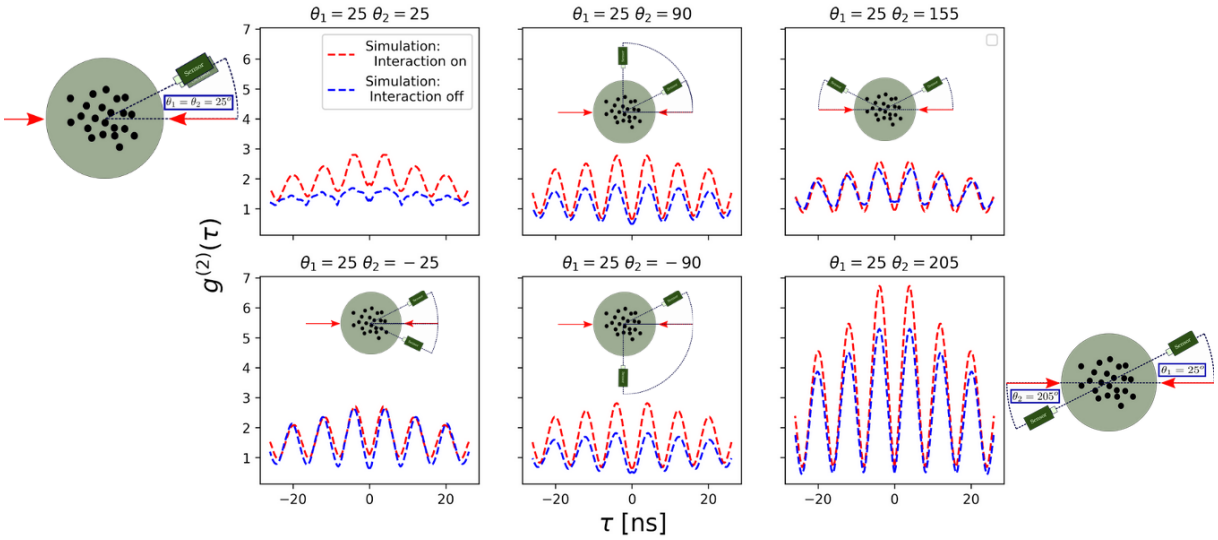

Figure 3 – $g^{(2)}(\tau)$ between different directions for $N = 5$ atoms, with $\Omega = 2\Gamma$ and $\Delta = 20\Gamma$ in a dilute atomic cloud ($b_0 = 0.1$). θ_1 and θ_2 refer to these directions, in spherical coordinates ($\phi = 0$). Correlations are stronger for the case of detectors placed at opposite directions as expected from FWM.

The largest spatial correlations are found at opposite directions as expected for biphotons in a FWM configuration (Figure 3). Moreover, in Figure 4(a) we focus on the opposite-detection case and report results that are consistent with the experimental data. The simulations (red/blue: with/without interaction) present a behavior similar to the experimental observations displayed in Figure 4(b). Also, the empirical fit (red-solid line), suggested by Araujo et al. to account for the collective effects, shows a χ coefficient larger than one, which is a witness of the presence of collective behavior. However, our simulations have maximum values of $g^{(2)}(\tau)$ larger than the experimental data. This problem is recurrent in our calculations. For instance, it appears again in the Cauchy-Schwartz inequality simulations (Figure 4(d)). Nonetheless, it probably is a consequence of the small number of atoms we can currently simulate. As we change the number of

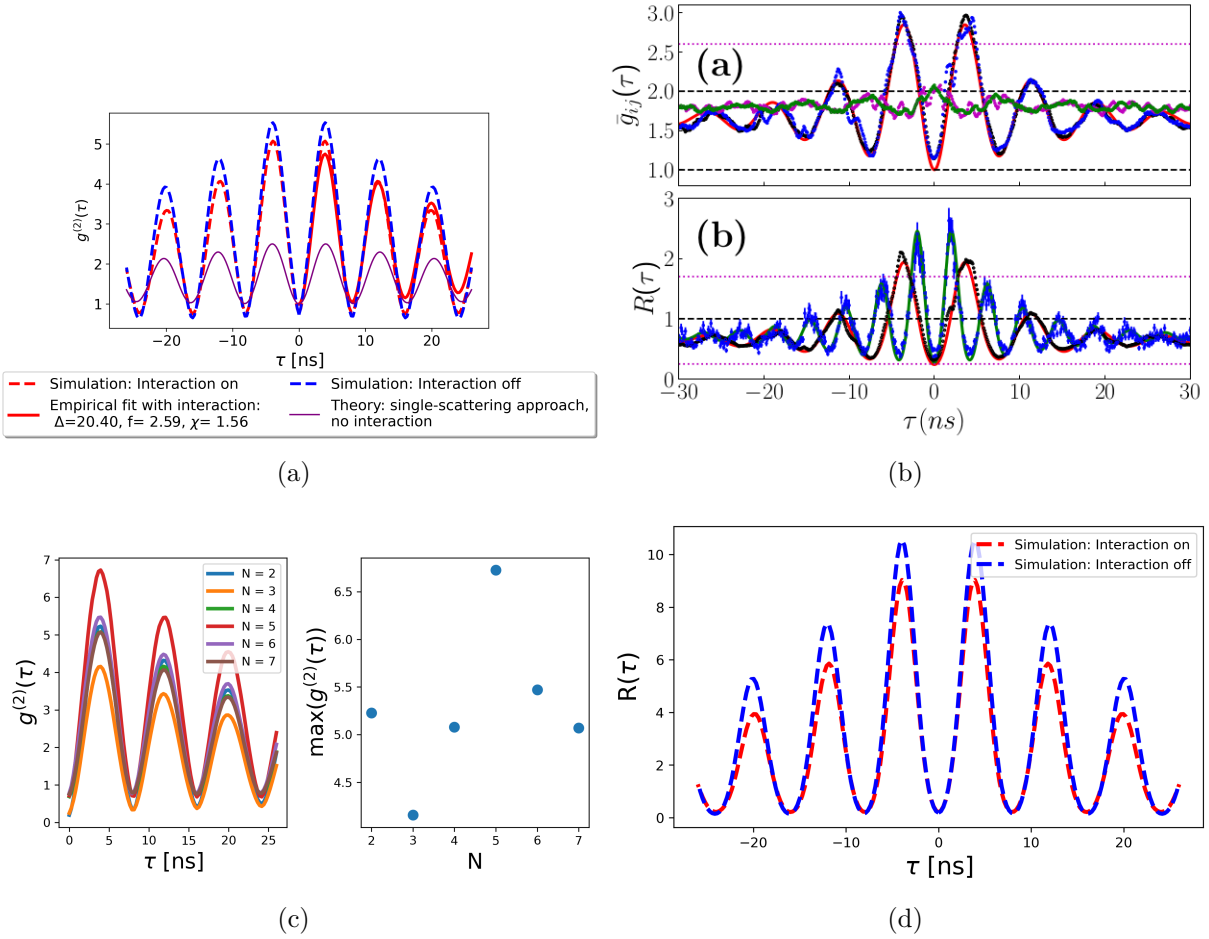

Figure 4 – (a) $g^{(2)}(\tau)$ for $N = 7$ in a dilute atomic cloud simulated considering: with interactions (red-dashed line), without interactions (blue-dashed line), the single independent atom model (purple line) and the empirical fit to account for collective effects (red-solid line). (b) Experimental observations from Ref [2], where the blue line in the first picture stands for the observed $g^{(2)}(\tau)$ in opposite directions with $\Omega = 2\Gamma$ and $\Delta = 20\Gamma$ and the second picture the corresponding Cauchy-Schwartz inequality. (c) $g^{(2)}(\tau)$ and $\max(g^{(2)}(\tau))$ for different number of atoms in a dilute atomic cloud. (d) Cauchy-Schwartz inequality for $N = 7$ atoms simulated by our model, turning on (red line) and off (blue line) the interactions.

particles ($2 < N < 7$), the maximum value changes without establishing a clear pattern (see Figure 4(c)). To account for this, we derived and implemented the analytical approach, described in Appendix B, that allows us to scale up the size of the system.

Furthermore, simulations with other optical densities, pump, and detuning conditions are available in the following table:

b_0	$\Omega = 0.02, \Delta = 0$	$\Omega = 1, \Delta = 0$	$\Omega = 2, \Delta = 20$
0.1	$g^{(2)}$, C-S	$g^{(2)}$, C-S	$g^{(2)}$, C-S
3		$g^{(2)}$, C-S	$g^{(2)}$, C-S
5		$g^{(2)}$, C-S	$g^{(2)}$, C-S

Table 1 – Hyperlinks to web folders with the corresponding simulation results.

The computer program made for the simulations is **available and documented** on this repository.

3.2 Single and double excitation subspace simulations

3.2.1 Benchmarking

To verify our analytical approach, we compare, for a specific set of atomic positions, $\langle \sigma_i^- \rangle = \beta_i(t)$ and $\langle \sigma_i^- \sigma_j^- \rangle = \beta_{ij}(t)$, calculated from the expectation values of our exact (scalar) simulations, to the coefficients obtained after solving the differential equations 2.8 and 2.9. In Figures 5(c) and 5(d), we show the results of both methods for different sizes of the atomic cloud ($b_0 = 0.1$ and 3) demonstrating the accuracy of our approximation in the weak-drive regime. As can be seen, our approximated approach is able to correctly reproduce the exact model results.

Moreover, in Figures 5(e) and 5(f) we also compare the $g^{(2)}_{\mathbf{R}_1,\mathbf{R}_2}(0)$ quantity for different directions when $\mathbf{R}_1$ is fixed at 25^o. The correlation function is obtained from exact simulations (scalar and vector models) and the subspace approach (Equation 2.10). Overall, the subspace simulations are able to replicate the behavior of the exact scalar equations.

3.2.2 Large systems

An important advantage of the subspace approach is that we are able to simulate systems of $N > 100$ in a few hours whereas, with the exact simulations, it is impossible to calculate clouds with more than $N = 7$ atoms with our computational resources. In Figure 6(a), we show the time necessary to calculate $g^{(2)}(0)$ for different second detector directions and how long it takes to solve the differential equations (2.8) and (2.9) as we increase the number of atoms. We show the case of $N = 40$ (black circle) in Figure 6(b), showing stronger correlations in opposite directions.

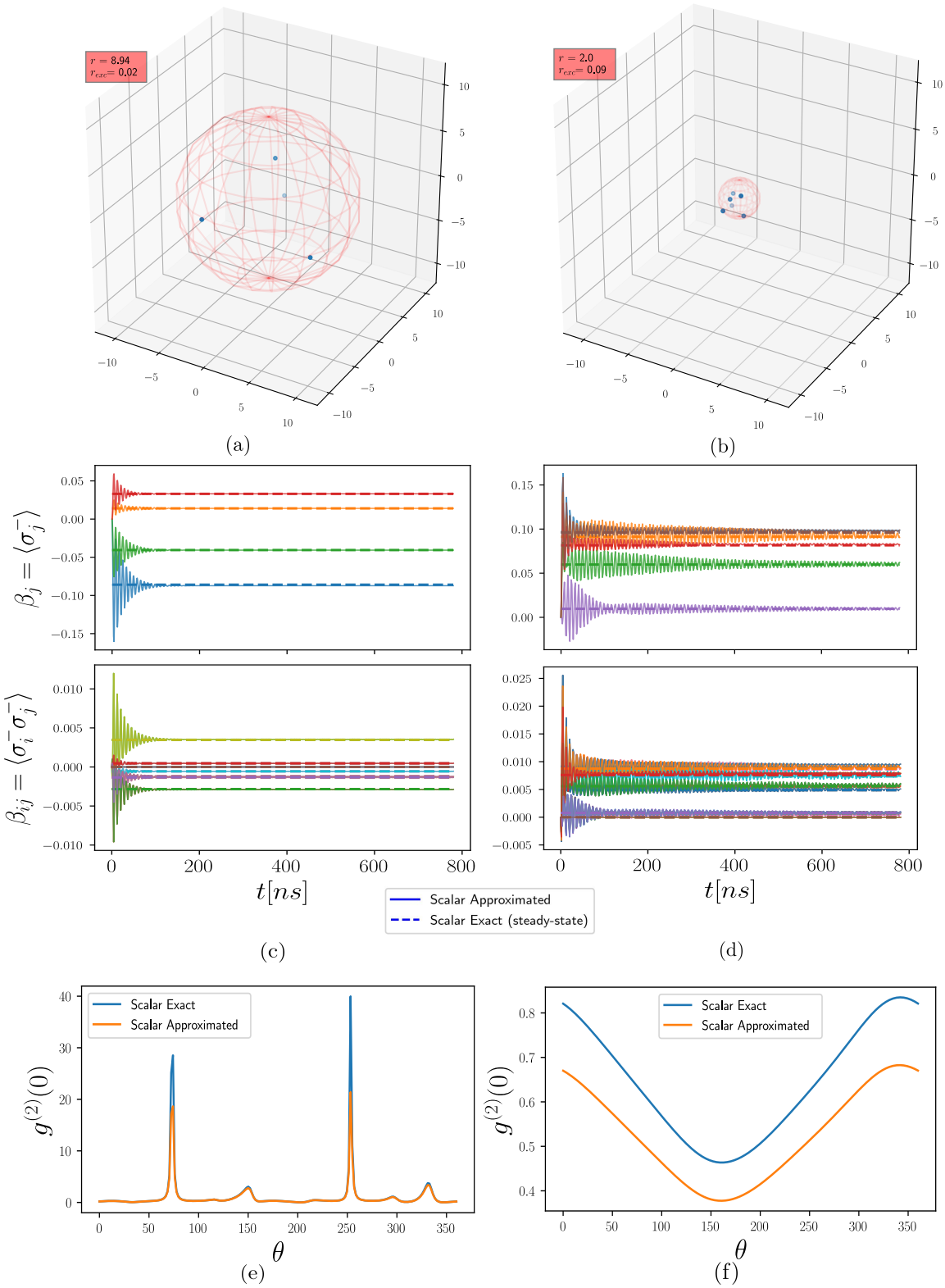

Figure 5 – Left (right) column corresponds to a specific simulation with $b_0 = 3$ (0.1), $N = 4$ (6), $\Omega = 2\Gamma$ and $\Delta = 20\Gamma$. (a) and (b): Geometric representation of the simulated atomic cloud. (c) and (d) In the second/third row, the values of $\beta_j(t) = \langle \sigma_j \rangle$ and $\beta_{ij}(t) = \langle \sigma_i \sigma_j \rangle$ are simulated using the subspace approach [solid lines] and the expectation value of the steady-state from the exact scalar model [dashed lines]. (e) and (f): Second-order correlation function for $\tau = 0$ with the first detector fixed at $\theta_1 = 25$ and changing the angle θ of the second sensor. Simulations are evaluated using the exact scalar (blue line) and the subspace approach (orange line).

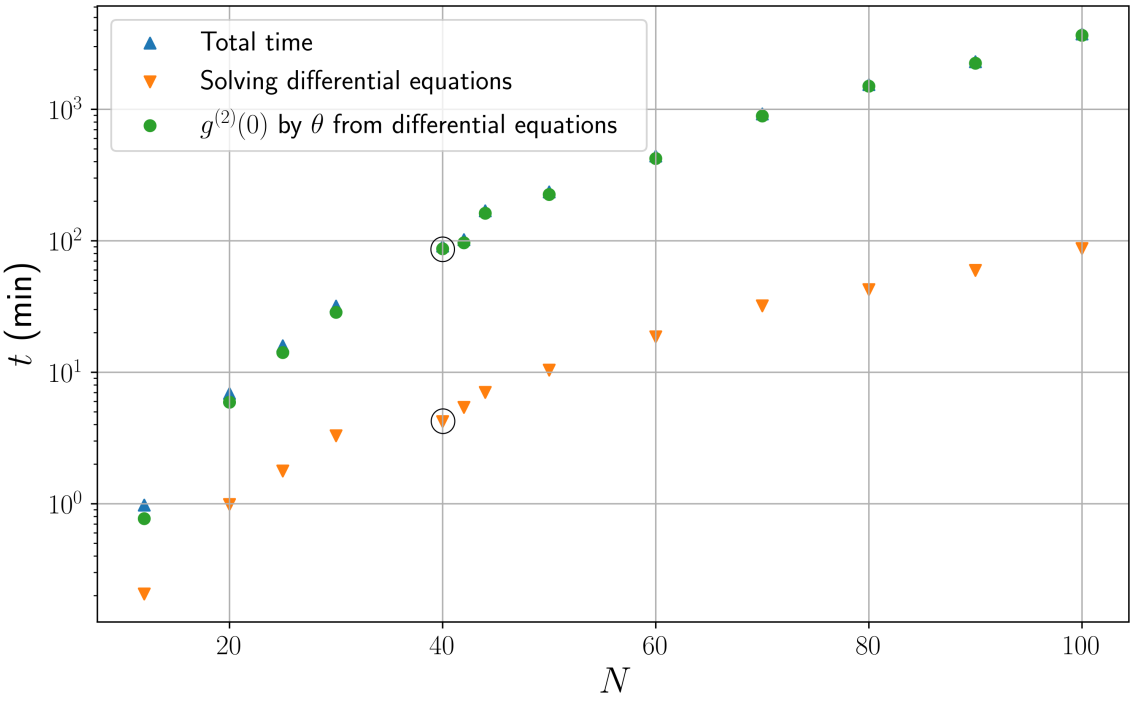

(a)

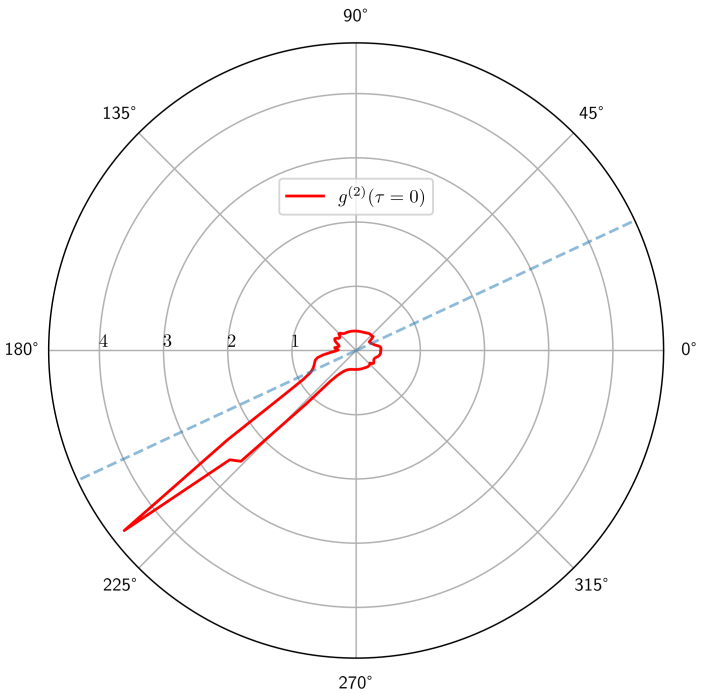

(b)

Figure 6 – (a) Time to: solve differential equations (2.8) and (2.9) (yellow triangles), obtain $g^{(2)}(0)$ from Equation 2.10 for 200 different angles (green circles), and complete the simulation (blue triangles). (b) Polar plot of $g^{(2)}(\tau = 0)$ for the $N = 40$ (black circle of (a)) case. $\theta_1 = 25°$ is the direction of the first detector (blue-dashed line).

4 Conclusion

Overall, we showed that considering dipole-dipole interaction in a four-wave-mixing configuration enables us to obtain results consistent with experimental data. In other words, this approach captures the experimental stronger correlations in opposite directions and demonstrates a second-order correlation behavior similar to the laboratory observations with collective effects. Moreover, the simulations considering the single- and double-excitation subspace correctly replicate the exact approximation in the weak-drive regime. This method is not only limited to the FWM configuration of this work and can be applied to other situations where there is interest in two excitations. For instance, in studying the contributions of an extra photon in light localization (eigenvalues analysis) [30]. Furthermore, using the quantum regression theorem, we plan to derivate and implement the second-order correlation function for the subspace approach. These simulations will allow us to characterize and investigate the collective effects for systems with a large number of atoms in a possible future master's project.

References

1 ASIMOV, I. Isaac Asimov Asks,"How Do People Get New Ideas?". MIT Technology Review, oct. 2014. Available on: <https://www.technologyreview.com/2014/10/20/169899/isaac-asimov-asks-how-do-people-get-new-ideas/>.

2 ARAÚJO, M. O.; MARINHO, L. S.; FELINTO, D. Observation of Nonclassical Correlations in Biphotons Generated from an Ensemble of Pure Two-Level Atoms. *Physical Review Letters*, v. 128, n. 8, p. 083601, feb. 2022. Available on: <https://link.aps.org/doi/10.1103/PhysRevLett.128.083601>.

3 KIMBLE, H. J. The quantum internet. *Nature*, v. 453, n. 7198, p. 1023–1030, jun. 2008. ISSN 1476-4687. Available on: <https://www.nature.com/articles/nature07127>.

4 REN, J.-G. et al. Ground-to-satellite quantum teleportation. *Nature*, v. 549, n. 7670, p. 70–73, sep. 2017. ISSN 1476-4687. Available on: <https://www.nature.com/articles/nature23675>.

5 BENNETT, C. H.; DIVINCENZO, D. P. Quantum information and computation. *Nature*, v. 404, n. 6775, p. 247–255, mar. 2000. ISSN 1476-4687. Available on: <https://www.nature.com/articles/35005001>.

6 BRIDA, G.; GENOVESE, M.; BERCHERA, I. R. Experimental realization of sub-shot-noise quantum imaging. *Nature Photonics*, v. 4, n. 4, p. 227–230, apr. 2010. ISSN 1749-4893. Available on: <https://www.nature.com/articles/nphoton.2010.29>.

7 LUGIATO, L. A.; GATTI, A.; BRAMBILLA, E. Quantum imaging. *Journal of Optics B: Quantum and Semiclassical Optics*, v. 4, n. 3, p. S176–S183, apr. 2002. ISSN 1464-4266. Available on: <https://doi.org/10.1088/1464-4266/4/3/372>.

8 KWIAT, P. G. et al. New High-Intensity Source of Polarization-Entangled Photon Pairs. *Physical Review Letters*, v. 75, n. 24, p. 4337–4341, dec. 1995. Available on: <https://link.aps.org/doi/10.1103/PhysRevLett.75.4337>.

9 RUBIN, M. H. et al. Theory of two-photon entanglement in type-II optical parametric down-conversion. *Physical Review A*, v. 50, n. 6, p. 5122–5133, dec. 1994. Available on: <https://link.aps.org/doi/10.1103/PhysRevA.50.5122>.

10 HALDER, M. et al. Entangling independent photons by time measurement. *Nature Physics*, v. 3, n. 10, p. 692–695, oct. 2007. ISSN 1745-2481. Available on: <https://www.nature.com/articles/nphys700>.

11 ORTIZ-GUTIÉRREZ, L. et al. Experimental Fock-State Superradiance. *Physical Review Letters*, v. 120, n. 8, p. 083603, feb. 2018. Available on: <https://link.aps.org/doi/10.1103/PhysRevLett.120.083603>.

12 BALIĆ, V. et al. Generation of Paired Photons with Controllable Waveforms. *Physical Review Letters*, v. 94, n. 18, p. 183601, may 2005. Available on: <https://link.aps.org/doi/10.1103/PhysRevLett.94.183601>.

13 MATSUKEVICH, D. N. et al. Entanglement of a Photon and a Collective Atomic Excitation. *Physical Review Letters*, v. 95, n. 4, p. 040405, jul. 2005. Available on: <https://link.aps.org/doi/10.1103/PhysRevLett.95.040405>.

14 ZHAO, B. et al. A millisecond quantum memory for scalable quantum networks. *Nature Physics*, v. 5, n. 2, p. 95–99, feb. 2009. ISSN 1745-2481. Available on: <https://www.nature.com/articles/nphys1153>.

15 ALBRECHT, B. et al. Controlled Rephasing of Single Collective Spin Excitations in a Cold Atomic Quantum Memory. *Physical Review Letters*, v. 115, n. 16, p. 160501, oct. 2015. Available on: <https://link.aps.org/doi/10.1103/PhysRevLett.115.160501>.

16 MITCHELL, M. W.; HANCOX, C. I.; CHIAO, R. Y. Dynamics of atom-mediated photon-photon scattering. *Physical Review A*, v. 62, n. 4, p. 043819, sep. 2000. Available on: <https://link.aps.org/doi/10.1103/PhysRevA.62.043819>.

17 DU, S. et al. Four-Wave Mixing and Biphoton Generation in a Two-Level System. *Physical Review Letters*, v. 98, n. 5, p. 053601, jan. 2007. Available on: <https://link.aps.org/doi/10.1103/PhysRevLett.98.053601>.

18 OLIVEIRA, R. A. de et al. Single-Photon Superradiance in Cold Atoms. *Physical Review A*, v. 90, n. 2, p. 023848, aug. 2014. Available on: <https://link.aps.org/doi/10.1103/PhysRevA.90.023848>.

19 ARAÚJO, M. O. et al. Superradiance in a Large and Dilute Cloud of Cold Atoms in the Linear-Optics Regime. *Physical Review Letters*, v. 117, n. 7, p. 073002, aug. 2016. ISSN 1079-7114.

20 DICKE, R. H. Coherence in Spontaneous Radiation Processes. *Physical Review*, v. 93, n. 1, p. 99–110, jan. 1954. Available on: <https://link.aps.org/doi/10.1103/PhysRev.93.99>.

21 CIDRIM, A. et al. Photon Blockade with Ground-State Neutral Atoms. *Physical Review Letters*, v. 125, n. 7, p. 073601, aug. 2020. Available on: <https://link.aps.org/doi/10.1103/PhysRevLett.125.073601>.

22 LEHMBERG, R. H. Radiation from an N-Atom System. I. General Formalism. *Physical Review A*, v. 2, n. 3, p. 883–888, sep. 1970. Available on: <https://link.aps.org/doi/10.1103/PhysRevA.2.883>.

23 FRIEDBERG, R.; HARTMANN, S. R.; MANASSAH, J. T. Frequency shifts in emission and absorption by resonant systems ot two-level atoms. *Physics Reports*, v. 7, n. 3, p. 101–179, mar. 1973. ISSN 0370-1573. Available on: <https://www.sciencedirect.com/science/article/pii/037015737390001X>.

24 STEPHEN, M. J. First-Order Dispersion Forces. *The Journal of Chemical Physics*, v. 40, n. 3, p. 669–673, feb. 1964. ISSN 0021-9606. Available on: <https://aip.scitation.org/doi/10.1063/1.1725188>.

25 JEN, H.-H. *Collective Light Emission: Many quantum emitters*. [S.l.]: Institute of Physics Publishing, 2020.

26 FRIEDBERG, R.; MANASSAH, J. T. Analytic expressions for the initial Cooperative Decay Rate and Cooperative Lamb Shift for a spherical sample of two-level atoms. *Physics Letters A*, v. 374, n. 15, p. 1648–1659, apr. 2010. ISSN 0375-9601. Available on: <https://www.sciencedirect.com/science/article/pii/S0375960110001726>.

27 MEYSTRE, P.; SARGENT, M. *Elements of Quantum Optics*. [S.l.]: Springer Science & Business Media, 2007. ISBN 9783540742111.

28 LOUDON, R. *The Quantum Theory of Light*. [S.l.]: OUP Oxford, 2000. ISBN 9780191589782.

29 JOHANSSON, J. R.; NATION, P. D.; NORI, F. QuTiP 2: A Python framework for the dynamics of open quantum systems. *Computer Physics Communications*, v. 184, n. 4, p. 1234–1240, apr. 2013. ISSN 0010-4655. Available on: <https://www.sciencedirect.com/science/article/pii/S0010465512003955>.

30 FAYARD, N. et al. Many-body localization in waveguide quantum electrodynamics. *Phys. Rev. Research*, American Physical Society, v. 3, p. 033233, Sep 2021. Available on: <https://link.aps.org/doi/10.1103/PhysRevResearch.3.033233>.

31 OSTERMANN, L. et al. *Collective radiation of coupled atomic dipoles and the precise measurement of time*. (PhD Thesis), Innsbruck, 2016. Available on: <https://resolver.obvsg.at/urn:nbn:at:at-ubi:1-4909>.

32 FICEK, Z.; TANAS, R. Entangled states and collective nonclassical effects in two-atom systems. *Physics Reports*, v. 372, n. 5, p. 369–443, dec. 2002. ISSN 03701573. ArXiv: quant-ph/0302082. Available on: <http://arxiv.org/abs/quant-ph/0302082>.

APPENDIX A – Dipole-dipole interaction: derivation outline

Many derivations of the coupled dipole model exist in the literature, from the older pioneering works done by Refs. [22, 23, 24] to more modern ones [25, 31, 32]. Here we will briefly outline the derivation conducted in Ref. [31].

Consider N two-level identical atoms fixed at positions $\mathbf{r}_1, \mathbf{r}_2, ..., \mathbf{r}_N$. In the electric dipole approximation, the field is assumed to be uniform over the whole atom. Consequently, the contribution of the atoms, field and the interaction give the following Hamiltonian:

$$\begin{aligned} H &= H_{Atom} + H_{Field} + H_{Interaction} \\ &= \omega_0 \sum_{i=1}^{N} \sigma_i^+ \sigma_i^- + \sum_{\mathbf{k},\lambda} \omega_k a_{\mathbf{k},\lambda}^\dagger a_{\mathbf{k},\lambda} + - \sum_{i=1}^{N} \mathbf{d}_i \cdot \mathbf{E}\left(\mathbf{r}_i\right). \end{aligned}$$

ω_0 represents the frequency between $|g\rangle$ and $|e\rangle$, ω_k the frequency of the kth mode and $\mathbf{d}_i$ the dipole moment of the ith dipole. The contribution from the interaction can be written in the second quantization formalism as,

$$H_{Interaction} = i \sum_{i=1}^{N} \sum_{\mathbf{k},\lambda} g_{\mathbf{k},\lambda} \left[a_{\mathbf{k},\lambda} \exp\left(i\mathbf{k}\mathbf{r}_i\right) - \text{ h.c. } \right] \left(\sigma_i^+ + \sigma_i^-\right).$$

with $g_{\mathbf{k},\lambda} = \sqrt{\omega_k / 2\epsilon_0 V}\, \mathbf{e}_{\mathbf{k},\lambda} \cdot \mu$. We have assumed that the atomic transition dipoles moments all have an equal orientation and amplitude (i.e. $\mu_i = \mu$). Now, we shall calculate the dynamics of the operators. First, we calculate the time evolution of $a_{\mathbf{k},\lambda}$ using Heisenberg equation $\partial_t a_{\mathbf{k},\lambda} = i\left[H, a_{\mathbf{k},\lambda}\right]$, which leads to

$$\begin{aligned} a_{\mathbf{k},\lambda}(t) &= a_{\mathbf{k},\lambda}\left(t_0\right) \exp\left(-i\omega_k \left(t - t_0\right)\right) \\ &\quad - \int_{t_0}^{t} \mathrm{d}t' \exp\left(-i\omega_k \left(t - t'\right)\right) g_{\mathbf{k},\lambda} \sum_{i=1}^{N} \exp\left(-i\mathbf{k}\mathbf{r}_i\right) \underbrace{\left(\sigma_i^+ + \sigma_i^-\right)}_{\sigma_i^x} \left(t'\right). \end{aligned} \tag{A.1}$$

Similarly, we can calculate the dynamics of an arbitrary atomic operator O solving its corresponding Heisenberg equation,

$$\partial_t O = i[H, O] = i\omega_0 \sum_{i=1}^{N} \left[\sigma_i^+ \sigma_i^-, O\right] - i \sum_{i=1}^{N} \left[\mathbf{d} \cdot \mathbf{E}\left(\mathbf{r}_i, t\right), O\right], \tag{A.2}$$

and substitute $a_{\mathbf{k},\lambda}$ given by Equation A.1. Now, the final objective is to simplify the differential equation A.2 and replace O by ρ, obtaining the evolution of the density matrix. To simplify the differential equation, we follow the steps below:

1. Introduce normal ordering for photon creator and annihilator operators.
2. Replace the sum over all modes by an integral, i.e. , $\sum_{\mathbf{k},\lambda} \to V/(2\pi)^3 \int \mathrm{d}^3\mathbf{k}$
3. We perform the Markov approximation, i.e., $\sigma_i^+(t') + \sigma_i^-(t') \to \sigma_j^+(t)\exp(i\omega_0(t'-t)) + \sigma_j^-(t)\exp(-i\omega_0(t'-t))$
4. Integrate over solid angles and perform rotating-wave approximation (neglect fast-oscillating terms).

We obtain:

$$\begin{aligned}\partial_t O = & i\sum_i \left[\left(\omega_0 - \Omega_{ii}^+\right)\sigma_i^+(t)\sigma_i^-(t) - \Omega_{ii}^-\sigma_i^-(t)\sigma_i^+(t), O(t)\right] \\ & + i\sum_{i\neq j}\left[\Omega_{ij}\sigma_i^-(t)\sigma_j^+(t), O(t)\right] \\ & + \frac{1}{2}\sum_{i,j}\Gamma_{ij}\Big(2\sigma_i^+(t)O(t)\sigma_j^-(t) \\ & -\sigma_i^+(t)\sigma_j^-(t)O(t) - O(t)\sigma_i^+(t)\sigma_j^-(t)\Big),\end{aligned}$$

which can be simplified as $\partial_t\rho = i[\rho, H] + \mathcal{L}[\rho]$ where Γ_{ij} and Ω_{ij} are the same given by Equation 2.4. Notice that Γ_{ij} couples the atoms through the vacuum field so that the spontaneous emission from each atom influences the spontaneous emission from the other. On the other hand, the interaction term Ω_{ij} introduces a coherent coupling between the atoms.

APPENDIX B – Single and double excitation subspace dynamics: derivation

Considering Equation 2.1, we can rewrite (2.2) and (2.3) as

$$\mathcal{H}(\hat{\rho}) = -\frac{i}{\hbar}\sum_{n=1}^{N}\left[H_n, \rho(t)\right] - i\sum_{n\neq m,m}^{N}\Delta_{nm}\left[\sigma_n^+\sigma_m^-, \rho(t)\right], \tag{B.1}$$

$$\mathcal{L}(\hat{\rho}) = \frac{1}{2}\sum_{n,m=1}^{N}\Gamma_{mn}\left[2\sigma_n^-\rho(t)\sigma_m^+ - \left\{\sigma_m^+\sigma_n^-, \rho(t)\right\}\right]. \tag{B.2}$$

We take H_n from Equation 2.2

$$H = \sum_{n=1}^{N}\overbrace{-\hbar\frac{\Delta_n}{2}\sigma_n^z + \hbar\frac{\Omega_n}{2}\left(\sigma_n^+ + \sigma_n^-\right)}^{H_n} + \sum_{n\neq m,m}^{N}\hbar\Delta_{nm}\sigma_n^+\sigma_m^-, \tag{B.3}$$

with $\Omega_n = \Omega\left(e^{i\mathbf{k}\cdot\mathbf{r}_n} + e^{-i\mathbf{k}\cdot\mathbf{r}_n}\right)$, $\pm\sigma_j^z = 2\sigma_l^\pm\sigma_j^\mp - \mathbb{I}$ and $\Delta_n = \Delta$. We can define the subspace dynamics coefficients :

$$\beta_\ell(t) = \left\langle\sigma_\ell^-\right\rangle = \mathrm{tr}\left\{\rho(t)\sigma_\ell^-\right\} \quad \text{and} \quad \beta_{k\ell}(t) = \left\langle\sigma_k^-\sigma_\ell^-\right\rangle = \mathrm{tr}\left\{\rho(t)\sigma_k^-\sigma_\ell^-\right\}.$$

Before expanding the expressions, the following commutation relations between the operators are very useful:

$$\left\{\sigma_\ell^\pm, \sigma_j^\pm\right\} = 2\sigma_\ell^\pm\sigma_j^\pm, \quad \left[\sigma_\ell^\pm, \sigma_j^\pm\right] = 0, \tag{B.4}$$

$$\left\{\sigma_\ell^\pm, \sigma_j^\mp\right\} = 2\left(1-\delta_{\ell j}\right)\sigma_l^\pm\sigma_j^\mp + \delta_{\ell j}\mathbb{I}, \tag{B.5}$$

$$\left[\sigma_\ell^\pm, \sigma_j^\mp\right] = 2\sigma_\ell^\pm\sigma_j^\mp - 2\left(1-\delta_{\ell j}\right)\sigma_\ell^\pm\sigma_j^\mp - \delta_{\ell j}\mathbb{I} = 2\delta_{\ell j}\sigma_\ell^\pm\sigma_j^\mp - \delta_{\ell j}\mathbb{I} = \delta_{\ell j}\left[2\sigma_\ell^\pm\sigma_j^\mp - \mathbb{I}\right] = \pm\delta_{\ell j}\sigma_j^z, \tag{B.6}$$

$$\left[\sigma_\ell^z, \sigma_j^\pm\right] = \pm 2\delta_{\ell j}\sigma_j^\pm, \quad \left\{\sigma_\ell^z, \sigma_j^\pm\right\} = 2\left[\sigma_\ell^z\sigma_j^\pm \mp \delta_{\ell j}\sigma_j^\pm\right], \tag{B.7}$$

$$\left[\sigma_\ell^-, H_m\right] = \delta_{\ell m}\left[\sigma_\ell^-, H_\ell(t)\right]. \tag{B.8}$$

Then, for the single excitation case we have

$$\dot{\beta}_\ell(t) = \mathrm{tr}\left\{\dot{\rho}(t)\sigma_\ell^-\right\} = \mathrm{tr}\left\{\mathcal{H}[\rho(t)]\sigma_\ell^-\right\} + \mathrm{tr}\left\{\mathcal{L}[\rho(t)]\sigma_\ell^-\right\}. \tag{B.9}$$

For the second term,

$$\begin{aligned}
\mathrm{tr}\left\{\mathcal{L}[\rho(t)]\sigma_\ell^-\right\} &= \frac{1}{2}\sum_{n,m=1}^{N}\Gamma_{nm}\left[2\,\mathrm{tr}\left\{\sigma_n^-\rho(t)\sigma_m^+\sigma_\ell^-\right\} - \mathrm{tr}\left\{\left\{\sigma_m^+\sigma_n^-,\rho(t)\right\}\sigma_\ell^-\right\}\right] \\
&= \frac{1}{2}\sum_{n,m=1}^{N}\Gamma_{nm}\left[2\,\mathrm{tr}\left\{\sigma_n^-\rho(t)\sigma_m^+\sigma_\ell^-\right\} - \mathrm{tr}\left\{\sigma_m^+\sigma_n^-\rho(t)\sigma_\ell^- + \rho(t)\sigma_m^+\sigma_n^-\sigma_\ell^-\right\}\right] \\
&= \frac{1}{2}\sum_{n,m=1}^{N}\Gamma_{nm}\left[\mathrm{tr}\left\{\rho(t)\sigma_m^+\sigma_\ell^-\sigma_n^-\right\} + \mathrm{tr}\left\{\sigma_n^-\rho(t)\sigma_m^+\sigma_\ell^-\right\}\right. \\
&\quad \left. - \mathrm{tr}\left\{\sigma_n^-\rho(t)\sigma_\ell^-\sigma_m^+ + \rho(t)\sigma_m^+\sigma_n^-\sigma_\ell^-\right\}\right. \\
&= \frac{1}{2}\sum_{n,m=1}^{N}\Gamma_{nm}\left[\mathrm{tr}\left\{\sigma_n^-\rho(t)\left[\sigma_m^+,\sigma_\ell^-\right]\right\} + \mathrm{tr}\left\{\rho(t)\sigma_m^+\left[\sigma_\ell^-,\sigma_n^-\right]\right\}\right] \\
&= \frac{1}{2}\sum_{n,m=1}^{N}\Gamma_{nm}\,\mathrm{tr}\left\{\sigma_n^-\rho(t)\delta_{tm}\sigma_m^z\right\} \\
&= \frac{1}{2}\sum_{n=1}^{N}\Gamma_{nt}\,\mathrm{tr}\left\{\sigma_n^-\rho(t)\sigma_\ell^z\right\} \\
&= \frac{\Gamma_{\ell\ell}}{2}\,\mathrm{tr}\left\{\rho(t)\sigma_\ell^z\sigma_\ell^-\right\} + \frac{1}{2}\sum_{n\neq\ell}^{N}\Gamma_{nt}\,\mathrm{tr}\left\{\sigma_n^-\rho(t)\sigma_\ell^z\right\} \\
&= -\frac{\Gamma_{\ell\ell}}{2}\,\mathrm{tr}\left\{\rho(t)\sigma_\ell^-\right\} + \frac{1}{2}\sum_{n\neq\ell}^{N}\Gamma_{n\ell}\,\mathrm{tr}\left\{\sigma_n^-\rho(t)\sigma_\ell^z\right\}.
\end{aligned} \tag{B.10}$$

For the first term,

$$\begin{aligned}
\mathrm{tr}\left\{\mathcal{H}[\rho(t)]\sigma_\ell^-\right\} &= -\frac{i}{\hbar}\sum_{n=1}^{N}\mathrm{tr}\left\{\left[H_n(t),\rho(t)\right]\sigma_\ell^-\right\} - i\sum_{n\neq m,m}^{N}\Delta_{nm}\,\mathrm{tr}\left\{\left[\sigma_n^+\sigma_m^-,\rho(t)\right]\sigma_\ell^-\right\} \\
&= -\frac{i}{\hbar}\underbrace{\sum_{n=1}^{N}\mathrm{tr}\left\{H_n(t)\rho(t)\sigma_\ell^- - \rho(t)H_n(t)\sigma_\ell^-\right\}}_{T_1} \underbrace{-i\sum_{n\neq m,m}^{N}\Delta_{nm}\,\mathrm{tr}\left\{\left[\sigma_n^+\sigma_m^-,\rho(t)\right]\sigma_\ell^-\right\}}_{T_2}.
\end{aligned} \tag{B.11}$$

Expanding T_2 we have:

$$\begin{aligned}
T_2 &= \sum_{n\neq m,m}^{N} \Delta_{nm}\left[\mathrm{tr}\left\{\sigma_n^+\sigma_m^-\rho(t)\sigma_\ell^-\right\} - \mathrm{tr}\left[\rho(t)\sigma_n^+\sigma_m^-\sigma_\ell^-\right\}\right] \\
&= \sum_{n\neq \ell}^{N} \Delta_{n\ell}\left[\mathrm{tr}\left[\rho(t)\sigma_\ell^-\sigma_n^+\sigma_\ell^-\right\} - \mathrm{tr}\left[\rho(t)\sigma_n^+\sigma_\ell^-\sigma_\ell^-\right\}\right] \\
&+ \sum_{n\neq m,m\neq \ell}^{N} \Delta_{nm}\left[\mathrm{tr}\left\{\rho(t)\sigma_\ell^-\sigma_n^+\sigma_m^-\right\} - \mathrm{tr}\left[\rho(t)\sigma_n^+\sigma_m^-\sigma_\ell^-\right\}\right] \\
&= \sum_{n\neq m,m\neq \ell}^{N} \Delta_{nm}\left[\mathrm{tr}\left\{\rho(t)\sigma_\ell^-\sigma_n^+\sigma_m^-\right\} - \mathrm{tr}\left\{\rho(t)\sigma_n^+\sigma_\ell^-\sigma_m^-\right\}\right] \\
&= \sum_{n\neq m,m\neq \ell}^{N} \Delta_{nm}\,\mathrm{tr}\left\{\rho(t)\left[\sigma_\ell^-,\sigma_n^+\right]\sigma_m^-\right\} \\
&= \sum_{n\neq m,m\neq \ell}^{N} \Delta_{nm}\,\mathrm{tr}\left[\rho(t)\left(-\delta_{\ell n}\sigma_n^z\right)\sigma_m^-\right\} = -\sum_{m\neq \ell}^{N} \Delta_{lm}\,\mathrm{tr}\left\{\rho(t)\sigma_\ell^z\sigma_m^-\right\}.
\end{aligned} \tag{B.12}$$

And, for T_1, using (B.8) we have:

$$\begin{aligned}
T_1 = \sum_{n=1}^{N} \mathrm{tr}\left\{H_n\rho(t)\sigma_\ell^- - \rho(t)H_n\sigma_\ell^-\right\} &= \sum_{n=1}^{N} \mathrm{tr}\left\{\rho(t)\sigma_\ell^-H_n - \rho(t)H_n\sigma_\ell^-\right\} \\
&= \sum_{n=1}^{N} \mathrm{tr}\left\{\rho(t)\left[\sigma_\ell^-,H_n\right]\right\} \\
&= \mathrm{tr}\left\{\rho(t)\left[\sigma_\ell^-,H_\ell\right]\right\}.
\end{aligned} \tag{B.13}$$

We can simplify the trace as follows:

$$\begin{aligned}
T_1 = \mathrm{tr}\left\{\rho(t)\left[\sigma_\ell^-,H_l\right]\right\} &= \frac{1}{2}\,\mathrm{tr}\left\{\rho(t)\left[\sigma_\ell^-,-\Delta_\ell\hbar\sigma_\ell^z + \Omega_\ell\hbar\left(\sigma_\ell^+ + \sigma_\ell^-\right)\right]\right\} \\
&= -\frac{1}{2}\Delta_\ell\hbar\,\mathrm{tr}\left\{\rho(t)\left[\sigma_\ell^-,\sigma_\ell^z\right]\right\} + \frac{1}{2}\Omega_\ell\hbar\,\mathrm{tr}\left\{\rho(t)\left[\sigma_\ell^-,\left(\sigma_\ell^+ + \sigma_\ell^-\right)\right]\right\} \\
&= -\frac{1}{2}\Delta_\ell\hbar\,\mathrm{tr}\left\{\rho(t)\left[\sigma_\ell^-,\sigma_\ell^z\right]\right\} + \frac{1}{2}\Omega_\ell\hbar\,\mathrm{tr}\left\{\rho(t)\left[\sigma_\ell^-,\sigma_\ell^+\right]\right\},
\end{aligned} \tag{B.14}$$

and using the commutation relations we obtain:

$$\begin{aligned}
\mathrm{tr}\left\{\rho(t)\left[\sigma_\ell^-,H_\ell\right]\right\} &= -\frac{1}{2}\Delta_\ell\hbar\,\mathrm{tr}\left\{\rho(t)\left[\sigma_\ell^-,\sigma_\ell^z\right]\right\} + \frac{1}{2}\Omega_\ell\hbar\,\mathrm{tr}\left\{\rho(t)\left[\sigma_\ell^-,\sigma_\ell^+\right]\right\} \\
&= -\frac{1}{2}\Delta_\ell\hbar\,\mathrm{tr}\left\{2\rho(t)\sigma_\ell^-\right\} - \frac{1}{2}\Omega_\ell\hbar\,\mathrm{tr}\left\{\rho(t)\sigma_\ell^z\right\} \\
&= -\Delta_\ell\hbar\,\mathrm{tr}\left\{\rho(t)\sigma_\ell^-\right\} - \frac{1}{2}\Omega_\ell\hbar\,\mathrm{tr}\left\{\rho(t)\sigma_\ell^z\right\}.
\end{aligned} \tag{B.15}$$

Putting the Hamiltonian part together,

$$\begin{aligned}
\mathrm{tr}\left\{\mathcal{H}[\rho(t)]\sigma_\ell^-\right\} &= -\frac{i}{\hbar}\left(-\Delta_\ell\hbar\,\mathrm{tr}\left\{\rho(t)\sigma_\ell^-\right\} - \frac{1}{2}\Omega_\ell\hbar\,\mathrm{tr}\left\{\rho(t)\sigma_\ell^z\right\}\right) - i\left(-\sum_{m\neq\ell}^{N}\Delta_{(m}\,\mathrm{tr}\left\{\rho(t)\sigma_\ell^z\sigma_m^-\right\}\right) \\
&= i\left(\Delta_\ell\,\mathrm{tr}\left\{\rho(t)\sigma_\ell^-\right\} + \frac{1}{2}\Omega_\ell\,\mathrm{tr}\left\{\rho(t)\sigma_\ell^z\right\}\right) + i\sum_{m\neq\ell}^{N}\Delta_{\ell m}\,\mathrm{tr}\left\{\rho(t)\sigma_\ell^z\sigma_m^-\right\},
\end{aligned} \tag{B.16}$$

and adding the first and second terms of equation B.9, we obtain:

$$\beta_l(t) = \left(i\Delta_\ell - \frac{\Gamma_{\ell\ell}}{2}\right)\beta_l(t) + \frac{i}{2}\Omega_\ell \operatorname{tr}\left\{\rho(t)\sigma_\ell^z\right\} + \sum_{m\neq\ell}^{N} G_{\ell m} \operatorname{tr}\left\{\rho(t)\sigma_\ell^z\sigma_m^-\right\}, \tag{B.17}$$

where

$$G_{\ell m} = \Gamma_{\ell m}/2 + i\Delta_{\ell m}.$$

At last, if we consider that the number of atoms N in the system is much larger than the number atomic excitation N_{exc} , that is, the number of photons shared by the atoms, we can assume that each atom is almost in the ground state, which corresponds to $\operatorname{tr}\{\rho(t)\sigma_\ell^z\} \approx -1$ and $\operatorname{tr}\{\rho(t)\sigma_\ell^z\sigma_m^-\} \approx -\beta_m(t)$. This regime is valid when $\operatorname{tr}\{\rho(t)\sigma_m^-\} << 1$ for all m, such that $\operatorname{tr}\{\rho(t)\sigma_\ell^z\} \approx -1, \forall m$. In conclusion, we find the dynamics of the single excitation sector as

$$\dot{\beta}_\ell(t) = \left(i\Delta_\ell - \frac{\Gamma_{\ell\ell}}{2}\right)\beta_\ell(t) - \frac{i}{2}\Omega_\ell - \sum_{m\neq\ell}^{N} G_{\ell m}\beta_m(t).$$

A similar approach can be used for the β_{jm} coefficients of the double excitation part. Yielding, after approximations,

$$\begin{aligned}\dot{\beta}_{k\ell}(t) = \left[i\left(\Delta_k + \Delta_l\right) - \frac{1}{2}\left(\Gamma_{kk} + \Gamma_{lt}\right)\right]\beta_{k\ell}(t) - \frac{i}{2}\left(\Omega_t\beta_k(t) + \Omega_k\beta_t(t)\right) \\ - \sum_{m\neq\ell}^{N} G_{\ell m}\beta_{km}(t) - \sum_{m\neq k}^{N} G_{km}\beta_{ml}(t).\end{aligned} \tag{B.18}$$